Jurnal Mekanikal
June 2008, No. 25, 39 - 49

NUMERICAL SIMULATION OF A MICROCHIP COOLING WITH MICROJET ARRAY

Yeo Eng Soon, Normah Mohd. Ghazali*

Faculty of Mechanical Engineering,
Universiti Teknologi Malaysia,
81310 Skudai, Johor, Malaysia

ABSTRACT

The increasing demand for a more powerful microchip has projected power dissipation for high performance processor up to 300 Watts in 2018. With the dimensions expected to remain at 310 mm^2, the heat density approaches the limit of conventional cooling methods. Microjet impingement cooling is a potential solution for the thermal management of these high performance microchips. This study looks into the numerical simulation of microjet arrays impinging with nozzle diameter ranging from 40 μm to 76 μm. Simulation results show the ability of a single-jet with 76 μm diameter nozzle in cooling the microchip dissipating 4.3 Watts of heat flux over a 1 cm² area. For multiple jets array, simulation results show that it is capable of achieving very low average surface temperature. It has also identified the problem associated with the increased number of jets due to the cross flow between the jets. It is found that multiple jets have better performance than the single jet even though the flowrate per jet is much lower.

Keywords: *Microjet impingement, thermal management, heat transfer*

1.0 INTRODUCTION

According to the International Technology Roadmap for Semiconductors (ITRS), the increasing demand in recent years for a more powerful microchip has projected an increase in power dissipation from 149 Watts in 2003 to 300 Watts in 2018. Figure 1 shows this projected power dissipation for high performance processors [1].

Although the power dissipation is increasing, the dimensions of the processor are predicted to remain at 310 mm² and the junction temperature at 85 ºC [1]. As more transistors are to be fitted into the microchip, the heat density will increase. With extra heat generated at localized hotspots, the extraordinary high heat dissipation at hotspots will cause a sharp increase of the local temperature, which will damage the microchip. The finned and metallic heat sink can remove heat from the hot surface uniformly, but the extra heat from the hotspots will not be removed efficiently.

* Corresponding author: E-mail: normah@fkm.utm.my

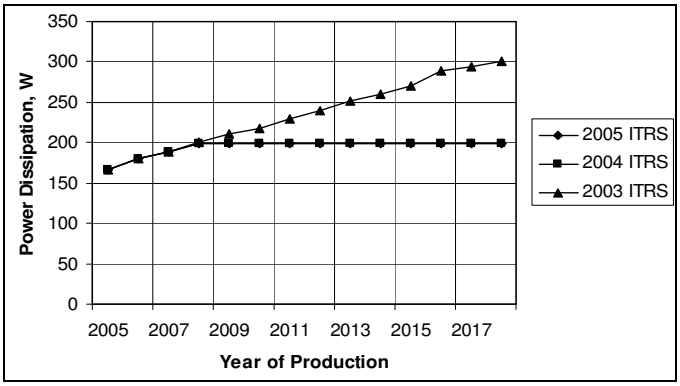

Figure 1: Power trend for a high performance processor

In the last three decades, numerous studies on macro jet impingement cooling have been done [2-5]. However, the studies were limited to macro scale impinging jets on the application such as the cooling of aircraft engines, automobile engines, and turbine blades. For these applications, the jet is impinging on the hot surface with a high velocity with a large nozzle size and wide gap between the nozzle and the surface to be cooled. As the velocity is high and the space between the nozzles and the surface is large, it is not applicable to the cooling of microchip. The high velocity of the jet directly impinging on the silicon chip surface will cause chip corrosion. Besides, with the high flow rate associated with a high velocity and a large nozzle size, a large pump will be required. The large size and noise generated make it not suitable for most of the applications where microchip cooling is required.

The study on microjet arrays has just begun in the recent years. The high heat transfer coefficient made it excellent in removing excessive heat from the microchip [6-9]. The light and small size of a microjet array enables it to be directly attached on top of the microchip, and thus eliminates the thermal resistance associated with finned and metallic heat sink. In situations where the contact between coolants and microchip is not allowed, a silicon layer is added.

Unlike in macro fluid flow study, the flow pattern in micro scale is hard to be investigated and examined through an experimental study. To examine the micro scale fluid flow, precise imaging instrument such as the micro Particle Image Velocimetry (PIV) imaging system is required. Even with complete instrumentation, it is not possible to study the cross flow patterns and heat transfer conditions at the impinging area. With the rapid increase in heat dissipation from microchip, a faster design cycle is needed. Numerical simulation using Computational Fluid Dynamics (CFD) code such as FLUENT, FEMLAB, CFD-ACE, FIDAP, COSMOSFloWorks etc. has made it possible to study microchip cooling by micro jet impingement.

2.0 COMPUTATIONAL MODELING

In this study, a commercial package of Computational Fluid Dynamics (CFD), FLUENT, is utilized to perform the numerical simulation of the heat transfer. Figure 2 shows a schematic of the actual microjet model. The simulations are done for a single jet, a 4-jet array, 9-jet array and a 13-jet array with the respective configurations given in Table 1. Figures 3 and 4 show schematic views with boundary conditions of the model. In the simulations, water is used as the medium of heat transfer and the surface of the microchip is made of pure silicon. The properties of liquid water and silicon are taken at 28.5 ºC and 1 atm.

The mass conservation equation used is [10]:-

$$\frac{\partial \rho}{dt} + \nabla \cdot (\rho \vec{v}) = 0 \tag{1}$$

where ρ is the density, t the time, and $\vec{v}$ the velocity vector. The first and second term on the left hand side are the change in density per unit time and the net inflow per unit time respectively.

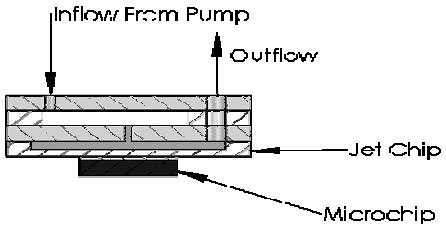

(a)

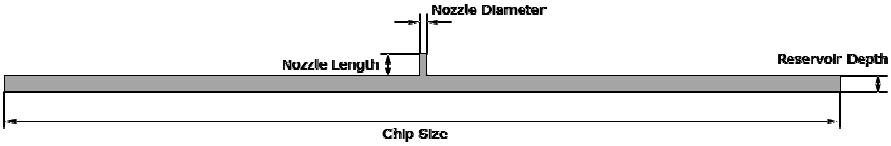

(b)

Figure 2: Cross sectional view of a) physical and b) simplified model

The momentum conservation equation used is:-

$$\frac{\partial}{\partial t}(\rho \vec{v}) + \nabla \quad (\rho \vec{v} \vec{v}) = \quad -\nabla p + \nabla(\bar{\bar{\tau}}) + \rho \vec{g} \tag{2}$$

with p being the static pressure, $\bar{\tau}$ is the stress tensor, and $\vec{g}$ the gravitational force. The first and second term on the left hand side is the momentum per unit time passing through fluid element and rate of change of momentum respectively. The first and second term on the right hand side are the rate of change of static pressure and rate of change of the stress tensor. $\rho\vec{g}$ is the gravitational body force.

Table 1: Summary of the physical parameters

Nozzle Length (mm)	Jet Diameter (μm)	Jet No.	Reservoir Depth (mm)	Chip Size (mm)	Space
0.3	76	1	0.2	11.284	Axisymmetric
0.5	76	1	0.2	11.284	Axisymmetric
0.7	76	1	0.2	11.284	Axisymmetric
0.3	65	1	0.2	11.284	Axisymmetric
0.3	60	1	0.2	11.284	Axisymmetric
0.3	50	1	0.2	11.284	Axisymmetric
0.3	40	1	0.2	11.284	Axisymmetric
0.3	76	1	0.2	10 (edge)	3D
0.3	76	4	0.2	10 (edge)	3D
0.3	76	9	0.2	10 (edge)	3D
0.3	76	13	0.2	10 (edge)	3D

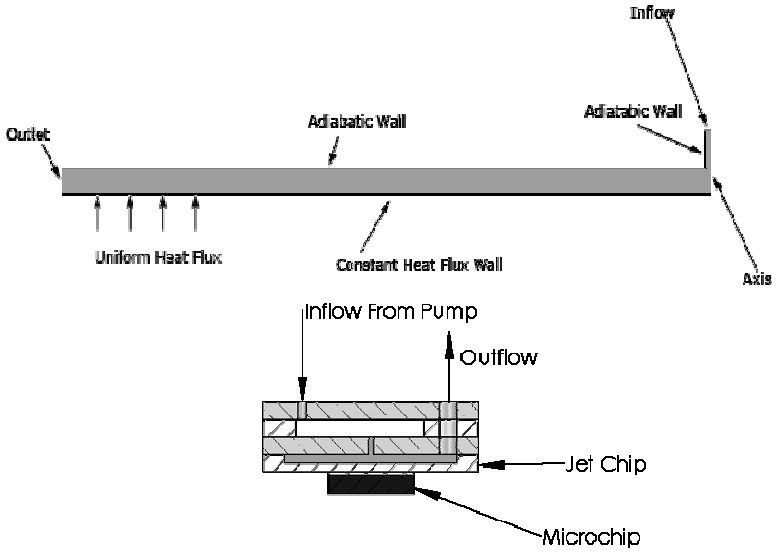

Figure 3: Simplified model of a single-jet. Inset: cross-sectional view

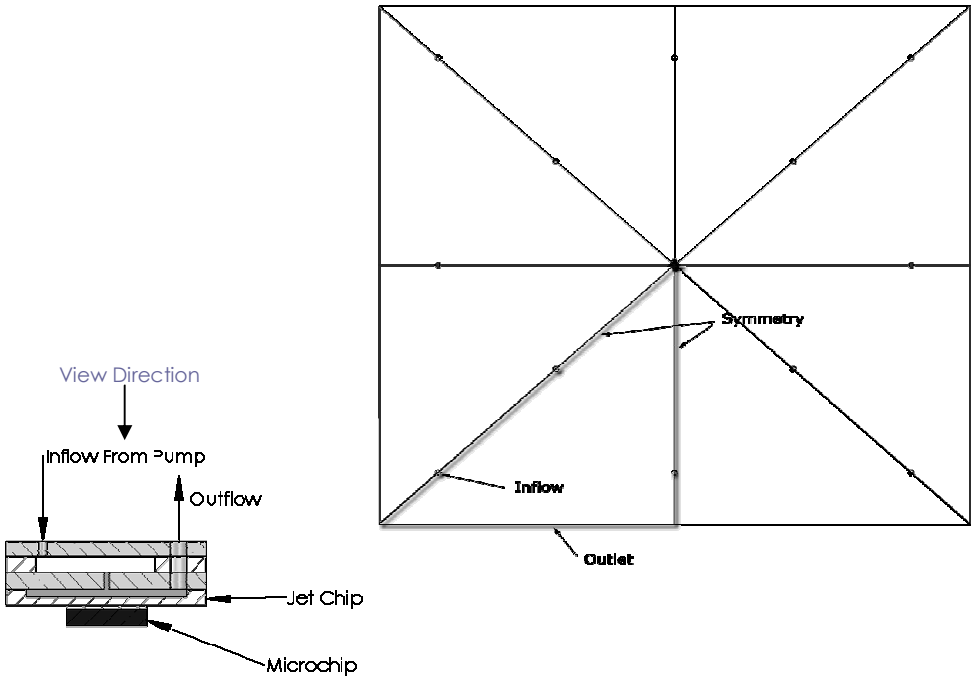

Figure 4: Simplified model of a $\frac{1}{8}$ model for a 13-jet microjet array. Inset: cross-sectional view

The Energy conservation equation used is:-

$$\frac{\partial}{\partial t}(\rho E) + \nabla \cdot (\vec{v}(\rho E + p)) = \nabla \cdot \left(k_{eff} \nabla T - \sum_j h_j \vec{J}_j + (\bar{\bar{\tau}}_{eff} \cdot \vec{v}) \right) \quad (3)$$

where is E the energy, T is temperature, k_{eff} the conductivity, h_j directional heat transfer coefficient, and $\vec{J}$ the specie vector. The first term on the left hand side describes the rate of change of energy stored within the control volume, the second and third term are the pressure work and kinetic energy term respectively. The three terms on the right hand side describe the energy transfer due to conduction, energy transfer due to species diffusion, and energy transfer due to viscous dissipation respectively.

The fluid is incompressible Newtonian fluid at steady-state condition with constant thermophysical properties. Assuming only convection heat transfer occurring within the adiabatic system, the edge is assumed large enough that back flow effect is negligible and thermal resistance between the chip and silicon surface has been neglected. The physical domain of the cooling space is then discretized into control volumes (meshes) with specified inlet velocity, outlet pressure, adiabatic wall, and constant heat flux. The momentum equations are first solved, followed by the continuity and the energy equations.

3.0 RESULTS AND DISCUSSION

The wall temperature is normalized to the impinging zone temperature [11]. The profiles for a microchip subjected to 4.3 W and 6.7 W power dissipation for both simulation and experimental results are shown in Figure 5. The experimental results by Wang et al. [7] were obtained through temperature measurements on a microchip surface away from the fluid.

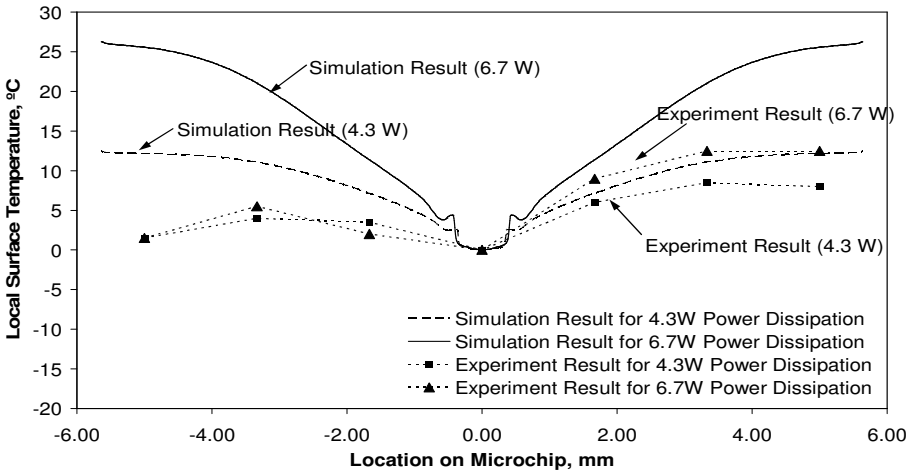

Figure 5: Normalized local surface temperature for both simulation and experimental results at power dissipation of 4.3 W and 6.7 W

In general, the simulation results show a similar trend with the experimental results. Both yield the lowest temperature at the impinging zone and the increasing temperatures towards the edge. The measured temperature dropped near the edge due to the heat loss. The measured temperature profile is not symmetrical with the temperature on the left hand side being lower than that on the right hand side. This is because the outlet of the experimental rig by Wang et al. is located at one side of the model. The presence of wall at the other sides confined the fluid flow in the lateral direction, therefore causing the unequal flow pattern and heat removal rate.

At the power dissipation of 4.3 W, the experimental result shows 8 ºC of temperature drop at the impinging zone compared to the edge located 5 mm away. The temperature drop was 12.2 ºC for the simulation results. The difference between the simulation and experimental results is 8.8 % based on the actual impinging zone temperature of 47.8 ºC. For the power dissipation of 6.7 W, the temperature drops for experimental and simulation results are 12.5 ºC and 25.6 ºC respectively. Based on the actual impinging zone temperature of 64 ºC, the difference is 20 %.

Figure 6 shows the velocity contour of a confined submerged jet with inlet velocity at 7.35 m/s. Upon entering the confined area, the jet diameter continually

decreases due to the interaction with the fluid inside the confined area. The jet then impinges on the microchip surface. At the impinging zone, a large pressure gradient occurred due to the presence of the impinging wall, it causes the fluid flow to divert. The largest pressure gradient occurred at the stagnation point, where the fluid velocity is zero.

When leaving the impinging zone, the fluid spread in a radial direction. Due to the interaction with the fluid in the confined area, the velocity of the fluid decreases as it propagates. Figure 7 shows the vector plot of the fluid jet.

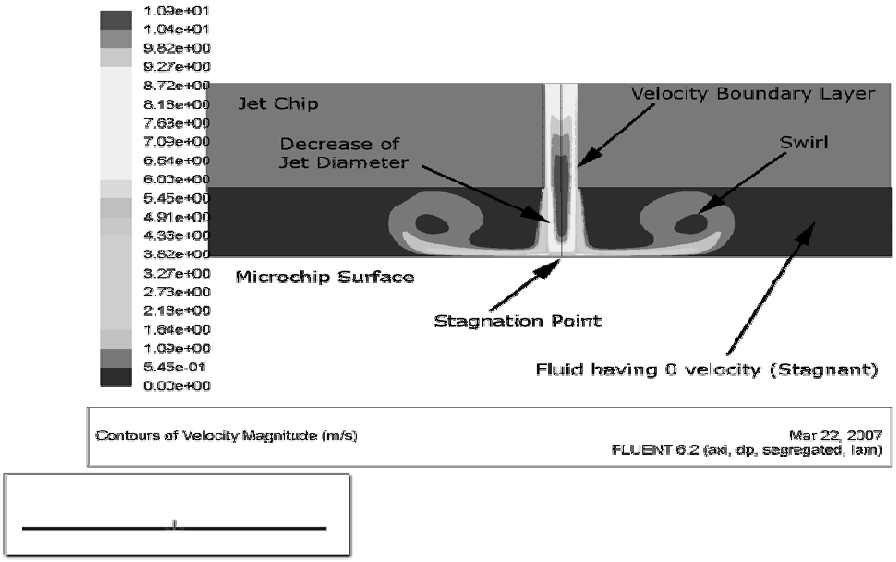

Figure 6: Velocity contour of a confined submerged jet with inlet velocity 7.35 m/s inset: front view of full scale simulation model

The effects of different parameters towards the performance of a microjet array, the volumetric flow rate-per-jet, number of jets, total volumetric flowrate, nozzle length, and nozzle diameter are investigated. The standard model used in the parametric studies is based on the model used by Wang et al. [7]. The parameters of the model are summarized in Table 2.

Figure 8 shows the comparison of the normalized average surface heat transfer coefficient between a single-jet and multiple-jet at different total volumetric flowrate. For the single-jet, the flowrate-per-jet is increased from 2 ml/min to 26 ml/min, whereas for the multiple-jet, flowrate-per-jet is maintained at 2 ml/min, but the number of jet is increased to increase the total flowrate. The average surface heat transfer coefficient is normalized based on the average surface heat transfer coefficient of a single-jet.

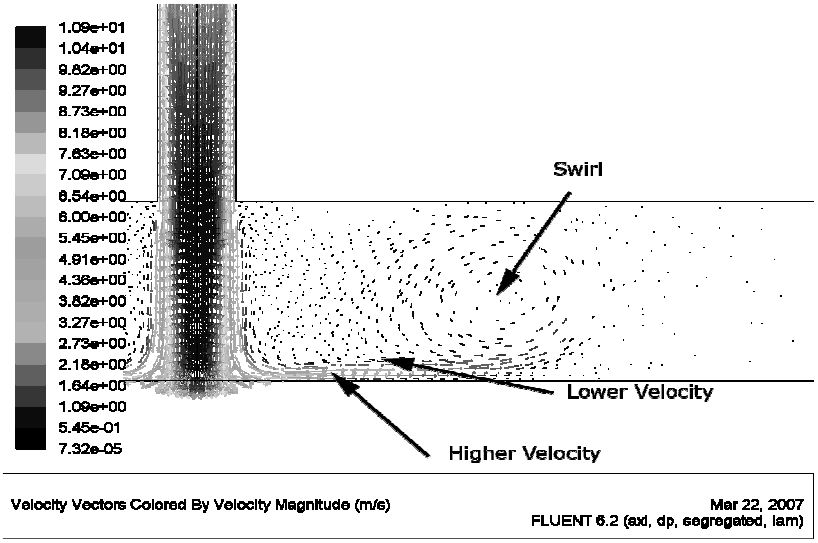

Figure 7: Velocity Vectors of a confined submerged jet with inlet velocity 7.35 m/s

Table 2: Parameters of the standard model

Parameters	Description
Jet Diameter	76 μm
Number of Jets	1
Nozzle Length	0.3 mm
Volumetric Flowrate	2 ml/min
Power Dissipation	4.3 W
Surface Area	1 cm²
Reservoir Depth	0.2 mm

The increase in volumetric flowrate from 2 ml/min to 26 ml/min for a single-jet will increase the average surface heat transfer almost linearly. While the nozzle diameter remains unchanged, when the volumetric flowrate is increased, the jet velocity will increase and therefore, increase the heat transfer coefficient. For a multiple-jet array, the volumetric flow rate of each jet is maintained at 2 ml/min and the number of jets is increased from a single-jet to 4-jet, 9-jet and 13-jet. The average heat transfer coefficient increases almost logarithmically with the increase of jet number. When the jet number increases from a single-jet to 4-jet, the increment of average heat transfer coefficient is large. However, when the jet number is increased from 9-jet to 13-jet, the increment is less. It shows that the presence of multiple-jet in the microjet array will increase the average heat

transfer coefficient, but will reduce the jet-efficiency for every jet probably due to cross flow effect.

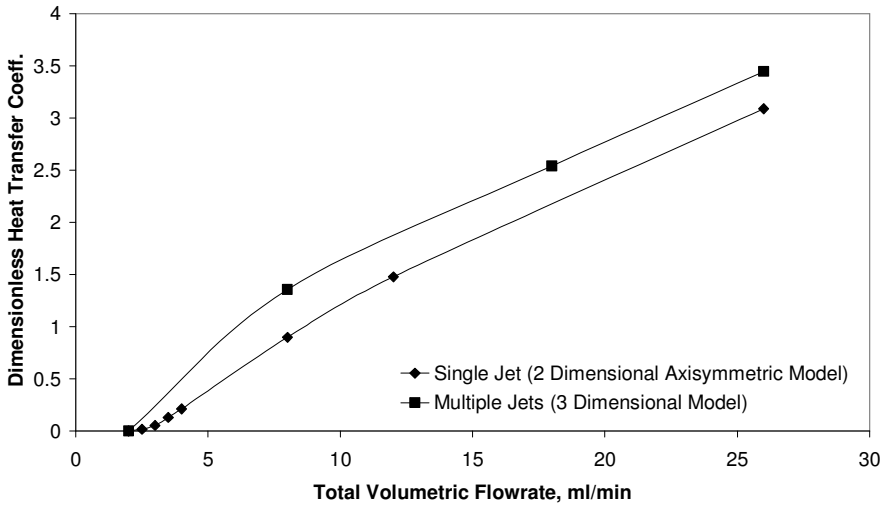

Figure 8: Comparison of the normalized average surface heat transfer coefficient of single-jet and multiple-jet

Comparing the average surface heat transfer coefficient between the single-jet and multiple-jet array, the average surface heat transfer coefficient for a multiple-jet is higher than a single-jet at equal total flowrate. Even though increasing the flowrate-per-jet will yield a higher inlet velocity and produce a better heat transfer coefficient, the area covered is still relatively small. When a multiple-jet is utilized, even though with a relatively lower heat transfer coefficient for every jet, more area is covered and therefore results in a higher heat transfer coefficient on average. An increase of almost 50 % was observed.

The effect on average surface heat transfer coefficient by the increment of nozzle length and diameter is shown in Figure 9. When the nozzle length is increased from 0.3 to 0.5 mm, the average surface heat transfer coefficient increases but decreases thereafter. It may be due to the increasing frictional force which reduces the kinetic energy of the fluid and impinging velocity in general. Therefore, it reduces the average surface heat transfer coefficient. The optimum nozzle length is found to be 0.55 mm, which yields the average heat transfer coefficient of 7200 W/m²·K.

The size of the impinging area relies largely on impinging velocity and jet diameter. When the nozzle diameter is increased from 40 μm to 50 % larger, the impinging area becomes larger due to the increased jet diameter. However, continually decreasing the jet diameter from the standard case is not possible to increase the jet velocity indefinitely. When the nozzle diameter becomes too small, the impinging area will decrease, causing the average heat transfer coefficient to

decrease. The optimum nozzle diameter is found to be 62 μm, yielding the average surface heat transfer coefficient 5800 W/m²·K.

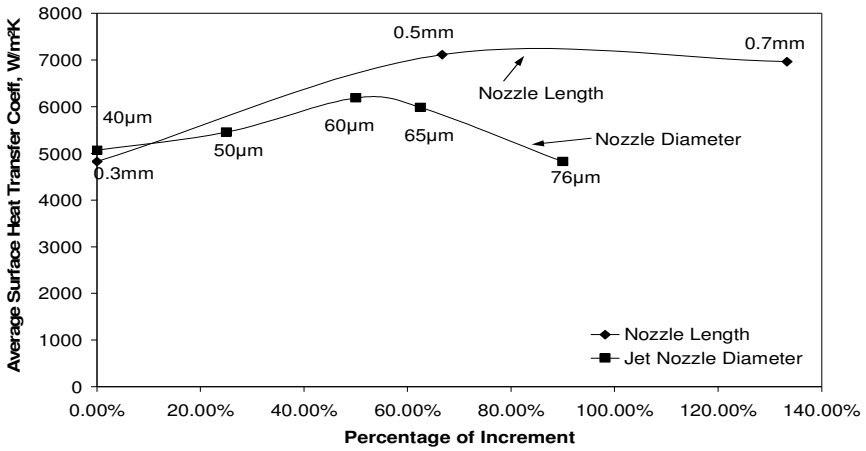

Figure 9: Effect on average surface heat transfer coefficient by increasing nozzle length and diameter

4.0 CONCLUSIONS

Simulation results show close agreement with experimental results obtained by Wang et al. [7] at the region close to the jet centre. The differences are due to difference between the rig set-up and the model. For a single-jet, when the volumetric flowrate is increased, the average surface heat transfer coefficient is increased. It is due to the increased impinging velocity, which yields a higher heat transfer coefficient on average. At equal flowrate, a multiple-jet array shows better performance than a single-jet in removing heat. When more jets are present, even though the jet efficiency is reduced, with the increase in the impinging area, the average heat transfer coefficient is increased. The optimum nozzle length and nozzle diameter for a 1 cm² microchip are 0.55 mm and 62 μm respectively. Microjet cooling array shows a good potential in removing excessive heat dissipated from the microchip. However, microjet array using liquid as coolant is still relatively new to the industry. More research has to be done before it can be commercialized. As hotspots are present in almost all microchips, the microjet cooling system for microchip with hotspots should be studied both numerically and experimentally to make the thermal management more efficient.

REFERENCES

1. Copeland, D., 2005. 64-bit Server Cooling Requirements, *Proceedings of 21st IEEE SEMI-THERM Symposium. IEEE.*
2. Krotzsch, S.G., 1968. *Wärme and Stoffübertragung bei Pallströmung aus Düsenund Blendenteldem*, New York: McGraw-Hill/Hemisphere Publishing.

3. Martin, H., 1977. Heat and Mass Transfer Between Impinging Gas Jets and Solid Surfaces, *Advances in Heat Transfer*, 13, 1-60.
4. Womac, D.J. ed, 1993. Correlating Equations for Impingment Cooling of SmallHeat Sources with Single Circular Liquid Jets, *ASME Journal of Heat Transfer*, 115, 106-115.
5. Angioletti, M., Nino, E. and Ruocco, G., 2005. CFD Turbulent Modeling of Jet Impingement and its Validation by Particle Image Velocimetry and Mass Transfer Measuremnets, *International Journal of Thermal Sciences*, 44, 349-356.
6. Stefanescu, S., Mehregany, M., Leland, J. and Yerkes, K., 1999. Micro Jet Array Heat Sink for Power Electronics, *Proceedings of the Twelfth IEEE International Conference on Micro Electro Mechanical Systems, MEMS*, 165-170.
7. Wang, E.N., Zhang, L., Koo, J-M, Maveety, J.G., Sanchez, E.A., Goodson, K.E. and Kenny, T.W., 2004. Micromachined Jets for Liquid Impingement Cooling for VLSI Chips, *J. Microelectromech. Sys.,* 13 (5), 833-842.
8. Fabbri, M., Jiang, S. and Dhir, V., 2003. Experimental Investigation of Single-Phase Micro Jets Impingement Cooling for Electronic Applications, *Proc. ASME Heat Transfer Conf., Las Vegas*, 1-8.
9. Fabbri, M., Jiang, S. and Dhir, V., 2005. A Comparative Study of Cooling of High Power Electronics Using Sprays and Microjets, *Trans. ASME,* 127, 38-48.
10. FLUENT. INC. 2005. *FLUENT 6.1 User's Guide*, Lebanon.
11. Yeo, E.S., 2007. Numerical Simulation of a Microchip Cooling System, *PSM Thesis*, Universiti Teknologi Malaysia, Skudai.